Origin of ultrafast annihilation effect of martensite aging: Atomistic simulations

Junkai Deng,[1,2] Xiangdong Ding,[1,3,*,†] Turab Lookman,[3] Tetsuro Suzuki,[2] Avadh Saxena,[3] Kazuhiro Otsuka,[2] Jun Sun,[1] and Xiaobing Ren[2,*,‡]

[1]*Multi-disciplinary Materials Research Center, Frontier Institute of Science and Technology, State Key Laboratory for Mechanical Behavior of Materials, Xi'an Jiaotong University, Xi'an 710049, China*

[2]*Ferroic Physics Group, National Institute for Materials Science, Tsukuba 305-0047, Ibaraki, Japan*

[3]*Theoretical Division, Los Alamos National Laboratory, Los Alamos, New Mexico 87545, USA*

(Received 29 July 2010; revised manuscript received 5 October 2010; published 1 November 2010)

Martensite aging effects, e.g., martensitic stabilization and rubberlike behavior, have attracted considerable attention in the past decades. It is known that martensite aging effects can be quickly eliminated once the aged martensite is brought into the parent phase even for a very short time, i.e., the annihilating effect of martensite aging (AEMA). However, the underlying mechanism of AEMA remains unclear due to the lack of an effective tool to probe the atomic processes during AEMA. It is unclear (1) whether AEMA is caused by a mere diffusionless transformation into the parent phase or by a diffusional process in the parent phase and (2) why long-time aging in martensite can be so easily eliminated in the parent phase. In this paper we use combined molecular-dynamics and Monte Carlo simulations to show that the origin of AEMA is related to atomic diffusion in the parent phase, not merely the reverse phase transformation. The open structure in the B2 parent phase and high-temperature result in a significantly higher diffusivity of point defects in the parent phase compared with that in the martensite; this explains the ultrafast annihilation of martensite aging. We attribute the driving force of AEMA to the symmetry-conforming short-range ordering tendency of point defects.

DOI: 10.1103/PhysRevB.82.184101 PACS number(s): 61.72.sh, 61.72.Bb, 64.60.De, 66.30.J−

I. INTRODUCTION

Many martensitic alloys exhibit a stabilization effect (i.e., an increase in the reverse martensitic transformation temperature) (Refs. 1–4) and a rubberlike behavior (i.e., a recoverable twinning deformation) (Refs. 4–6) after aging in the martensite state. Such martensite aging effects have attracted attention in the past decades from both scientifically and from the applications of shape memory alloys, where such effects need to be taken into account. There is also a well-observed conjugate phenomenon: the annihilation effect of martensite aging (AEMA), which refers to the very fast disappearance of martensite aging, once the aged martensite experiences a reverse transformation into the parent phase.[3,4] To be specific, martensitic stabilization means that martensite is more stable with aging so that the reverse-transformation finish temperature (A_f) increases with aging. However, once the stabilized martensite experiences a brief heating to the parent state (above the increased A_f) followed by cooling back to martensite state, the previous aging effect is completely removed and the system recovers the unaged martensite state with the A_f temperature restoring the unaged value. With further aging in the martensite state, martensitic stabilization reappears. As a brief heating to the parent phase can quickly eliminate martensite aging, AEMA has been routinely utilized to remove the martensite aging effect and to bring the sample into the fresh martensite state.

The underlying mechanism of AEMA has remained a puzzle so far, due to the lack of an effective tool to probe the atomic processes during AEMA. It is unclear whether AEMA is caused by a mere diffusionless transformation into the parent phase[7] or by a diffusional process in the parent phase.[4,8] Moreover, experimental observations also show that AEMA is complete even by soaking the sample to the parent state for a very short time;[4] e.g., in a Au-49.5 at. % Cd alloy, the martensite aging, which is built up over a rather long time of 5400 s at 298 K, can by simply erased by heating the sample to the parent phase (at 324 K) and soaking for only a few tens of seconds.[4] It is noted that the relative small difference in the martensite aging temperature (298 K) and parent aging temperature (324 K) cannot fully account for such a large difference in the martensite aging rate and its annihilation rate. It is unclear why the aging effect, accumulated over a long time in the martensite state, can be so easily eliminated in the parent phase.

In this work we try to answer these questions by a combination of molecular-dynamics (MD) and Monte Carlo (MC) simulations which we have previously used to reproduce martensitic stabilization.[9] We first reproduce AEMA by this hybrid atomistic approach and our analysis further reveals that the fast recovery of short-range configurations of point defects is responsible for AEMA. That is, the AEMA behavior is caused by the diffusion of point defects in the parent phase, not by a mere diffusionless martensitic (or reverse phase) transformation. Through the calculation of average diffusion coefficient of point defects in both martensite and the parent phase, we find that the mobility of point defects is related to both crystal structures and the temperature of the system. The open structure in the B2 parent phase and high temperature make the diffusivity of point defects in the parent phase much higher than that in the martensite. This leads to the fast annihilation of martensite aging. Finally, we propose that the thermodynamic driving force for atomic diffusion in the parent phase arises from the requirement of symmetry-conforming short-range ordering of point defects.

The layout of this paper is as follows. In Sec. II, we introduce the simulation method and procedure. Section III presents the simulation results where we investigate the variation in A_f during martensite aging process and the sub-

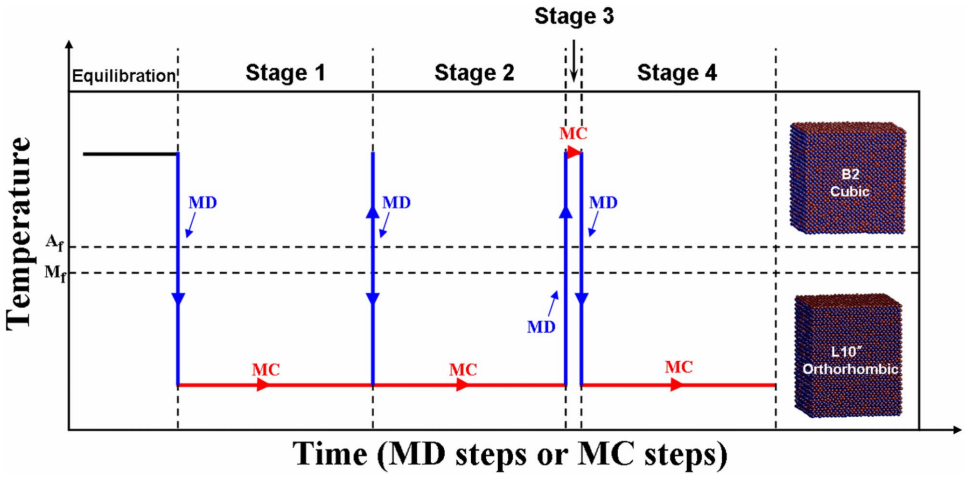

FIG. 1. (Color online) Schematic illustration of the whole atomic simulation procedure. In the equilibration stage the system is held in the parent state for sufficient time to establish an equilibrium state of the parent phase. Stage 1 denotes the martensite aging process, where the well-aged parent phase was quenched to get a fresh martensite and then aged in martensite. In stage 2, the system first experiences a "flash" martensite-parent phase-martensite transformation cycle (i.e., no aging is performed in the parent phase) and the martensite formed by this flash treatment is aged again. In stage 3, the system is heated up to the parent phase and then aged for a short time in the parent phase. In stage 4, the aged parent phase in stage 3 is cooled down to martensite and the subsequent martensite is aged again.

sequent deaging or annihilation process, in relation to the possible change in short-range order (SRO) and long-range order (LRO). In Sec. IV, we then discuss the kinetic and thermodynamic reasons for the fast annihilation of martensite aging in the parent phase and Sec. V summarizes our main results.

II. SIMULATION METHOD AND PROCEDURE

As AEMA involves both diffusionless martensitic (or reverse phase) transformation and possible diffusional aging and deaging process, we use a combination of MD and MC methods in the present study. The "fast" martensitic transformation is studied by MD simulations and the "slow" atomic diffusion process during aging/deaging is simulated by the MC method. Such a method has been used to simulate martensitic stabilization effect in our previous work,[9] and has proved to be effective. Details of this method should be referred to in Ref. 9.

Since it is experimentally known that both AEMA and martensite aging effects are strongly dependent on point defects,[4,10] we established a $A_{55}B_{45}$-type B2 structural binary alloy as our model material in which 5 at. % of A atoms were introduced in the β sublattice (occupied by B atoms) as the antisite point defects (ASDs). The initial unit cell with B2 structure was constructed in a cubic box containing 221 184 atoms (121 652 A atoms and 99 532 B atoms). To avoid the existence of a free surface, periodic boundary condition was imposed in all three dimensions of the supercell.

To clarify whether the origin of AEMA behavior is merely related to the diffusionless transformation into the parent phase or caused by a diffusional process in the parent phase, we design our simulation procedure as shown in Fig. 1. Stage 1–2, where no parent phase diffusion is allowed (as the soaking time in the parent phase is 0 ps), is to test if a mere reverse transition to the parent phase can erase the martensite aging established in stage 1; stage 3–4, where the system is allowed to stay in the parent phase for a short period of time, is to test if diffusion in the parent phase is responsible for the annihilation of martensite aging.

To start our calculation, we use both MD and MC method to prepare a well aged or equilibrium parent phase at a relative temperature 0.54 (above A_f). In stage 1, we first cooled down this well-aged parent phase to a relative temperature 0.34 (below M_f) to obtain a fresh martensite (with MD), and then the system was allowed to evolve by MC to yield a well-aged martensite. In stage 2, we first up-quenched the well-aged martensite to the parent phase (at temperature 0.54) and immediately down-quenched to martensite (at temperature 0.34), and followed by another martensite aging stage. Through the change in A_f and the evolution of atomic distribution in stages 1 and 2, we can detect whether AEMA can occur by a mere diffusionless transformation. In stage 3, we first heat the well-aged martensite to the parent phase (at temperature 0.54) again. Instead of immediately cooling down as in stage 2, the parent phase was aged at temperature 0.54 for a short time. Finally, in stage 4 we cooled the aged parent phase down to martensite (at temperature 0.34) and then aged the martensite so obtained. Through monitoring the change in A_f and the evolution of the atomic distributions in stages 3 and 4, we can confirm whether AEMA is caused by the aging or diffusional process in the parent phase.

It is noted that among the above four stages, all the heating and cooling processes, or the diffusionless martensitic transformation processes, were simulated by MD method, and all the aging processes (the diffusional processes) were simulated by MC method. The MD calculations were based on the Parrinello-Rahman scheme,[11] and the isothermal-isobaric ensemble was adopted in the calculation. As there is no change in average structure during the aging process in both martensite and the parent phase,[6] canonical ensemble was used during the present MC simulation, which is based

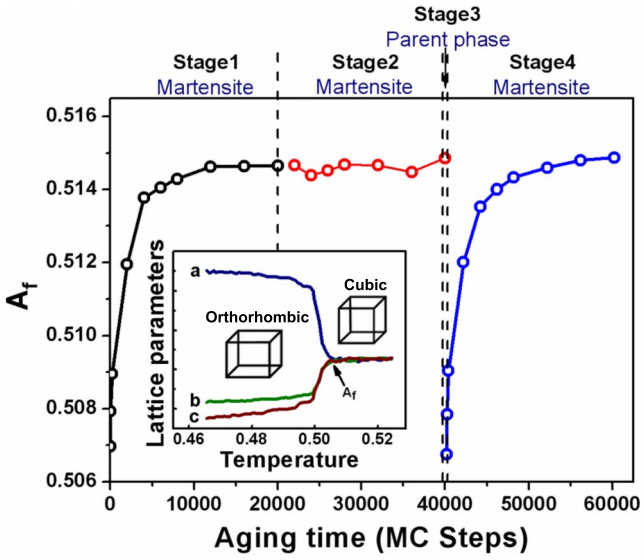

FIG. 2. (Color online) Variation in reverse transformation temperature (A_f) with aging time in martensite in stage 1, 2, and 4. The inset shows the reverse transformation from the orthorhombic structure to the cubic B2 structure and the definition of A_f temperature is from the results of MD calculation. The normalized temperature is used for A_f temperature here (see text for details).

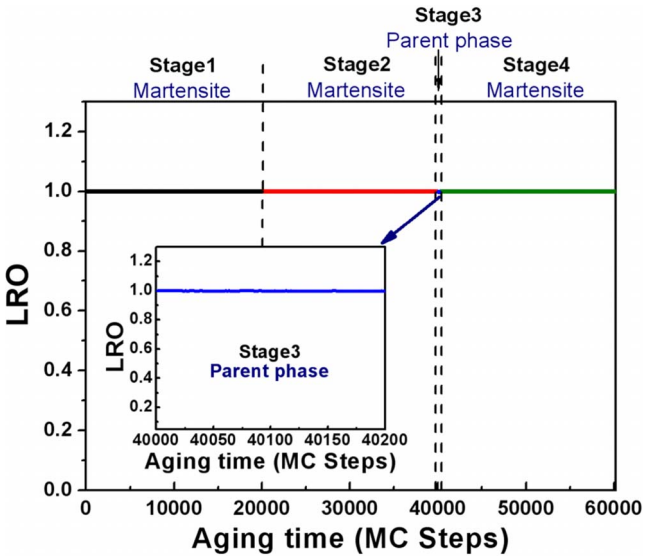

FIG. 3. (Color online) Variation in LRO with aging time during the whole simulation procedure.

on the classic Metropolis algorithm.[12] A simple 8-4 Lennard-Jones potential,[13] which has been successfully used to simulate a generic martensitic transformation (B2 to $L1_0''$, which is a pseudo-orthorhombic structure),[13–15] was used in both MD and MC simulations. Besides, the normalized temperature and lattice constants were applied for both MD and MC simulations.[16]

III. RESULTS

A. Detection of possible AEMA in two different processes: A mere reverse transformation and a reverse transformation with parent aging

As AEMA refers to the removal of martensite aging effect, we can detect the existence of AEMA by monitoring the change in A_f temperature relative to the unaged martensite. Based on the same method as in our previous work,[9] we can obtain the changes in A_f with aging in stages 1, 2, and 4, and the results are shown in Fig. 2. Stage 1 refers to the change in A_f of the fresh martensite with aging. The inset shows the reverse phase transformation involves a structure change from an orthorhombiclike structure to B2 structure. It is found that A_f increases with MC steps and saturates above 12 000 steps. This result is in good agreement with the well-observed martensitic stabilization in experiment.[17]

When the above well-aged martensite undergoes an abrupt up-quench to the parent phase followed by an immediate down-quench back to the martensite phase (i.e., avoid aging in the parent state), it is found that A_f of this "second stage martensite" keeps the same value as the well-aged martensite in the first stage, and further aging does not change this A_f, as shown in stage 2 of Fig. 2. This means that a mere diffusionless transformation cycle $L1_0''$-B2-$L1_0''$ cannot cause the AEMA.

Having confirmed that a mere diffusionless transformation cycle cannot cause the AEMA, we designed a diffusionless reverse transition plus a brief parent aging process, as shown in stage 3 of Fig. 1, where the well-aged martensite is up-quenched to the parent state and soaked for a short period of time and subsequently down-quenched to the martensite again and the A_f temperature of this newly formed martensite is monitored in stage 4 of Fig. 1. The result is shown in stage 4 of Fig. 2. We can clearly see that after aging in the parent phase for a short time (stage 3 in Fig. 1), martensite aging is eliminated: first, the A_f temperature almost restores the same value as that of the fresh martensite in stage 1; second, the A_f vs aging-time curve is quite similar to the martensitic stabilization of fresh martensite in stage 1, i.e., A_f increases with aging time in martensite and becomes saturated at long time (MC steps). Therefore, AEMA arises from the short-time aging in the parent phase (stage 3 of Fig. 2).

B. Atomic diffusion behavior during martensite aging and deaging process

From the above results it is clear that the AEMA is closely related to aging in the parent phase, not the phase transformation itself. This parent aging process that erases the martensite aging is usually called "deaging" process. Therefore, it is natural to ask what happens during this process at the atomic level. Clearly one can anticipate the parent aging is related to certain atomic diffusion process. For an ordered alloy such as B2 (the present case), atomic migration may cause two possible consequences: (1) a change in LRO parameter and (2) a change in SRO parameter.[18] Now we try to answer which one is responsible for the parent aging.

In the present work, LRO (Ref. 19) is defined as $L = \frac{r_\alpha - x_A}{1 - x_A}$, where r_α is the fraction of α sublattice occupied by appropriate atoms (A atoms); x_A is the mole fraction of atom A in the alloy. Figure 3 shows the evolution of LRO during the whole aging process in our simulation. It is clear that $L = 1$ and it does not change during the aging process (stages

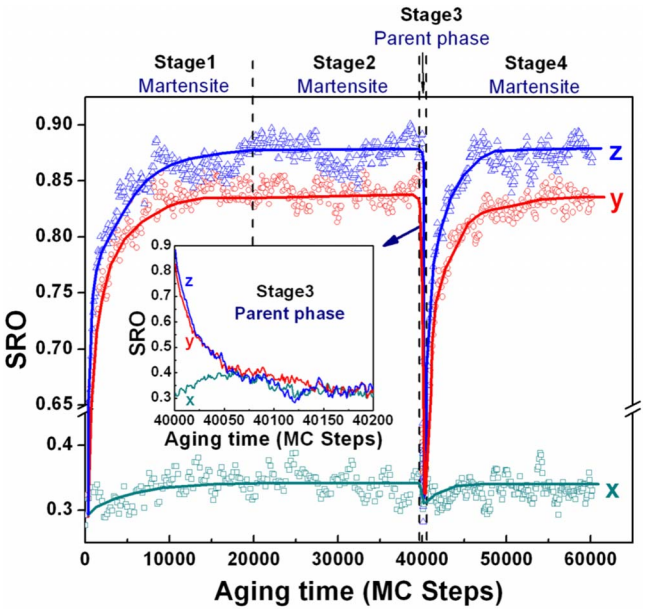

FIG. 4. (Color online) Variation in SRO with aging time during the whole simulation procedure. The values of SRO represent the short-range ordering of point defects at the nearest-neighbor sites along [100], [010], and [001] (x, y, and z directions, respectively).

1–4). This means that there is no change in the average structure during the process of both martensite aging (stage 1, 2, and 4) and the parent phase aging (stage 3). This result is also consistent with the experimental observation that no LRO change occurs during the aging process in both phases.[6] In addition, the lack of variation in LRO also indicates that the effective atomic diffusion only takes place within the same sublattice (β sublattice) of the ordered martensite, not between α and β sublattices. It can be further deduced that the diffusion of point defects within the β sublattice plays an important role in both martensite aging and AEMA behavior.

To denote the diffusion behavior of point defects in the β sublattice, we define the SRO (Ref. 20) as $s_{lmn}=1-\frac{P_i^{D|D}}{x_D}$, where *lmn* denotes the coordinates of the interatomic vector between sites i and j; the conditional probability $P_i^{D|D}$ is the probability to find an ASD at site i if there is an ASD at site j; x_D is the atomic fraction of ASDs. Figure 4 shows the evolution of SRO of point defects at the nearest sites along x, y, and z (i.e., [100], [010], and [001]) directions of the β sublattice with aging during the whole aging process.

Stage 1 of Fig. 4 shows the variation in defect SRO in fresh martensite with *martensite aging*. We found that the SRO vs aging time curve coincides with the A_f vs aging time curve (i.e., martensitic stabilization curve, stage 1 in Fig. 2). The initial values of defect SRO along x, y, and z directions are almost the same in fresh martensite; however, the SRO values along the above three directions gradually deviate and finally saturate at long aging time.

Stage 2 of Fig. 4 shows the SRO of the martensite that has experienced an abrupt diffusionless transformation cycle from a well-aged martensite (stage 2 or Fig. 1). It is noted that during such a diffusionless transformation cycle in stage 2, SRO remains unchanged from the previous value of the well-aged martensite (stage 1) and such a value does not change with *further martensite aging*. Such behavior coincides with constant A_f for stage 2 (Fig. 2). It means that a mere diffusionless transformation cycle does not change the SRO configurations of the well-aged martensite and hence does not eliminate the martensite aging effect.

Stage 3 of Fig. 4 refers to the evolution of SRO during *aging in the parent phase*. It is found that a short time ($\sim$100 MC steps) aging in the parent phase is sufficient to "rectify" the SRO that is established during much long aging (about 12 000 MC steps) in the martensite state and recover the SRO of the well-aged parent state (or fresh martensite). This indicates that the rearrangement (or diffusion) of point defects in the parent phase is much faster than that in the martensite state, being consistent with experiment.[4,8]

Stage 4 of Fig. 4 refers to the change in defect SRO in the *martensite phase after the system has experienced aging in the parent phase*. We found that the SRO curve coincides with the reestablishment of stabilization effect (stage 4 in Fig. 2). With aging in martensite, the SRO values along x, y, and z directions become different again, and finally saturate at large aging time. This is quite similar to that of martensite aging in fresh martensite. From the results in stages 3 and 4, we can further conclude that AEMA stems from the fast recovery of SRO state of point defects in the parent phase.

IV. DISCUSSION

A. Why can martensite aging effects be so easily eliminated in the parent phase?

The most interesting finding in the SRO evolution (Fig. 4) in comparison with the annihilation of martensite aging (Fig. 2) is that AEMA is associated with a very fast recovery of SRO to the equilibrium value of the parent phase. Compared with the equilibrium SRO of martensite which needs $>$12 000 MC steps to reach (i.e., the martensite aging process), the equilibrium SRO of the parent phase needs only $\sim$1/100 of the time to establish (i.e., the deaging process, stage 3 of Fig. 4). Such a big difference is consistent with well-known experimental fact that martensite aging usually requires hours or even days to establish but it can be simply removed by soaking the sample in the parent state for even tens of seconds. Now Fig. 4 tells that this ultrafast deaging effect is related to a fast evolution of SRO in the parent phase. Thus the central question is why the SRO evolution or diffusion can be so fast in the parent phase as compared with that in martensite state. In this section, we shall answer this question by calculating the average diffusion coefficient in both martensite and parent phase.

The conventional method of determining the atomic diffusion coefficient at thermal equilibrium through computer simulations is to observe the mean-square displacements (MSD) of tracer atoms.[21] The diffusion coefficient of one point defect can be estimated by observing the mean-square displacement as a function of time,[22]

$$D_d = \lim_{t\to\infty}\left[\frac{1}{6}\frac{\partial}{\partial t}R_d^2(t)\right], \quad (1)$$

where $R_d^2(t)$ represents the total mean-square displacement of this point defect after a time t. Since all point defects may be

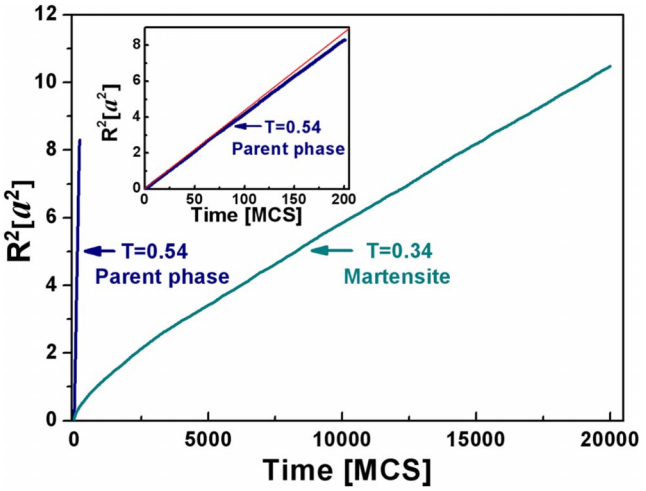

FIG. 5. (Color online) Average mean-square displacement of the point defects as a function of time (Monte Carlo steps, hereafter MCS). Relative temperature 0.54 corresponds to the parent phase with B2 cubic structure and relative temperature 0.34 corresponds to the martensite with orthorhombic structure, respectively.

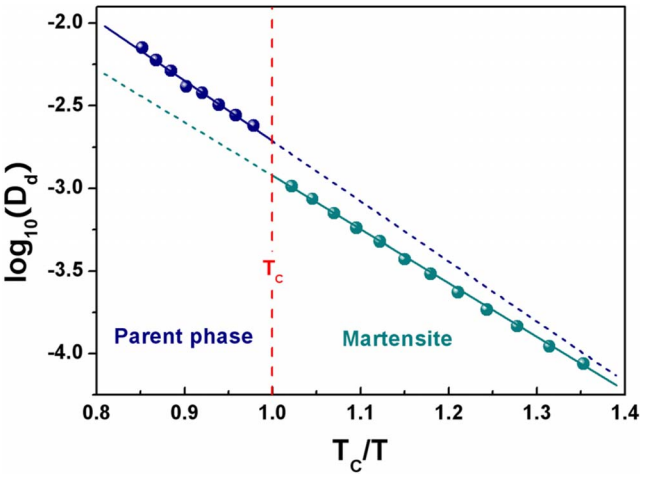

FIG. 6. (Color online) Arrhenius plots of the $\log_{10}(D_d)$ versus inverse temperature T_c/T for both parent phase and martensite; D_d (with units of $[a^2(\mathrm{MCS})^{-1}]$) is the average diffusion coefficient of point defects and $T_c=1/2(M_s+A_f)$ is the instability temperature of the parent phase.

viewed individually as tracers, the average diffusion coefficient of point defects is calculated in the same way from

$$D_d = \lim_{t\to\infty}\left(\frac{1}{6}\frac{\partial}{\partial t}\overline{R_d^2(t)}\right), \tag{2}$$

where $\overline{R_d^2(t)}$ denotes the average mean-square displacement of all the point defects at time t with

$$\overline{R_d^2(t)} = \frac{1}{N_d}\sum_{k=1}^{N_d} r_{d,k}^2. \tag{3}$$

Here N_d is the total number of point defects in the system, and $r_{d,k}^2$ is the mean-square displacement for the kth point defect, which can be described as

$$r_{d,k}^2 = |r_{d,k}(t) - r_{d,k}(0)|^2, \tag{4}$$

where $|r_{d,k}(t)-r_{d,k}(0)|$ is the vector distance traveled by the kth point defect over the traced time interval. We note that, the above method is also used to study the diffusion coefficient in an order-disorder transformation by means of MC methods,[21] and the determined diffusion coefficient of point defects is the average diffusion coefficient of the crystal in all directions.

Figure 5 shows the time evolution of the averaged mean-square displacement of the point defects $\overline{R_d^2(t)}$ in both martensite and the parent phase based on Eq. (3). Here, the mean-square displacement is scaled by the square lattice constant of B2 structure of parent phase (a^2) and the time is represented by number of MC steps (MCS). It is noted that there is a very large difference in the MSD curve between martensite and parent phase with parent phase showing a significantly faster diffusion rate than in the martensite. Although the difference in temperature (T=0.34 for martensite and T=0.54 for the parent phase) may partially account for such a difference, we shall show below that the structural difference between martensite and parent phase can create a big difference in the diffusivity and thus contribute a large part in very different rates between martensite aging and deaging (in the parent phase).

To compare the diffusivity in the parent phase with that in martensite, we calculated the diffusion coefficient of point defects at a given temperature by Eqs. (2)–(4). Since Eq. (2) is only valid in thermal equilibrium, we use the linear part of the MSD curves of Fig. 5 (which corresponds to the thermal equilibrium) to calculate D_d (diffusion coefficient of point defects) at different temperatures. The calculated $\log_{10} D_d$ vs T_c/T relation is shown in Fig. 6. It shows that the diffusion in both martensite and parent phase follows the standard Arrhenius relation of diffusion, $D_d=D_0\exp(-\Delta H/k_BT)$, where ΔH is the activation energy, k_B is the Boltzmann's factor, and D_0 is a prefactor related to attempt frequency and the intrinsic nature of a lattice.[23,24] The most notable result in Fig. 6 is that there exists a "jump" in the diffusivity at the transition temperature T_c, with a significant increase in the diffusivity when martensite is transformed into the parent phase. Clearly, this significant enhancement of diffusivity when martensite is transformed into the parent phase is largely responsible for the ultrafast AEMA or deaging. In addition to this structural effect on diffusivity, the high temperature in the parent phase also contributes to the fast AEMA or deaging, but it seems that the structure difference is the fundamental cause, as experimentally it has been found that martensite aging even near T_c (or M_s) is still significantly slower than the deaging (or parent phase aging).[4]

As D_0 and ΔH are independent of temperature, they are used to characterize the intrinsic diffusion ability of a system. Here we use these two parameters to quantify the difference in intrinsic diffusion ability between the parent phase and martensite. From the Arrhenius plot in Fig. 6, D_0 is found to be 9.57 $[a^2(\mathrm{MCS})^{-1}]$ and 2.27 $[a^2(\mathrm{MCS})^{-1}]$ for the parent phase and martensite, respectively; ΔH is found to be 3.91 and 3.47 for the parent phase and martensite, respectively. We note that the parent phase has a D_0 4.22 times as

large as that of martensite and has about 13% higher ΔH. Such a difference is likely to be related to the open and high-symmetry structure of the parent phase, where more equivalent sites exist, which results in more effective jumps of point defects. It is clear that such intrinsic difference in diffusion ability causes a discontinuous change in the diffusivity at martensite-parent transition temperature T_c.

B. Possible driving force for the diffusion of point defects during aging in the parent phase?

Our results showed that short-range redistribution of point defects during the parent phase aging is responsible for the ultrafast AEMA behavior. However, thermodynamically, it remains to be answered as to what is the driving force for such short-range-order redistribution of point defects in the parent phase. In this section, we will show that the driving force stems from a symmetry-conforming SRO (SC-SRO) tendency of point defects.[6,25]

The SC-SRO model states that the symmetry of short-range-order configuration of point defects should conform to the symmetry of the crystal lattice when in equilibrium. Accordingly, if the symmetry of short-range-order configuration of point defects does not follow the symmetry of crystal lattice, the free energy of the system will be high. To reduce the free energy of the system, point defects will exchange their positions in order to follow the symmetry of the crystal lattice.

For the well-aged martensite in the present calculation, the SRO values should be different in the [001], [010], and [100] directions as the structure of martensite is orthorhombic. When the well-aged martensite transforms into the parent phase, the SRO configurations of point defects are inherited by the parent phase due to the diffusionless phase transformation. However, according to the SC-SRO model, the inherent SRO configuration of point defects is not a stable configuration any more as the lattice symmetry of the parent phase becomes cubic. The symmetry difference between the SRO configuration of point defects and crystal lattice in the parent phase provides a driving force for the diffusion of point defects in the parent phase, which results in the AEMA behavior. A more detailed and quantitative analysis of the driving force for the AEMA will appear elsewhere.[26]

Interestingly, similar annihilation effect has been found not only in ferroelastic (martensite) materials but also in ferroelectric materials. The "deaging phenomenon" in ferroelectric materials shows that the ferroelectric phase aging effect can be eliminated by heating to the paraelectric state.[27] The origin of such annihilation of ferroelectric aging was also ascribed to the SC-SRO tendency of point defects.[28] Our simulations may also provide insight into the microscopic nature of the deaging phenomenon or "annihilation effect" in ferroelectric materials.

V. CONCLUSION

In conclusion, we have investigated the AEMA by a combination of molecular-dynamics and Monte Carlo methods. We reach the following conclusions.

(1) AEMA arises from an ultrafast parent phase aging (or called deaging) process, which involves the diffusion of point defects; it is not caused by a mere diffusionless transformation.

(2) The ultrafast AEMA process stems from a fast recovery of the short-range-order configuration of point defects of the parent phase to its equilibrium SRO configuration; no long-range-order change is involved during AEMA.

(3) The origin of ultrafast AEMA is related to a significantly enhanced diffusion rate in the parent phase as compared with that in martensite, together with a high aging temperature compared with martensite aging. The open and high-symmetry structure of the B2 parent phase may be responsible for the fast diffusion rate in the parent phase.

(4) The thermodynamic driving force for the AEMA behavior can be explained by the SC-SRO microscopic model.

ACKNOWLEDGMENTS

The authors are grateful to Y. Wang and Z. Zhang for stimulating discussions. This work was supported by KAKENHI (X.R.), NSFC (Grants No. 50771079 and No. 50720145101), the 973 Program of China (Grant No. 2010CB631003) and 111 project of China (Grant No. B06025) as well as the support from the U.S. DOE at LANL (Grant No. DE-AC52-06NA25396).

*Author to whom correspondence should be addressed.
†dingxd@mail.xjtu.edu.cn
‡ren.xiaobing@nims.go.jp

[1] A. Abu Arab and M. Ahlers, Acta Metall. **36**, 2627 (1988).
[2] R. Santamarta, C. Seguí, J. Pons, and E. Cesari, Scr. Mater. **41**, 867 (1999).
[3] J. Van Humbeeck, J. Janssen, N. Mwamba, and L. Delaey, Scr. Metall. **18**, 893 (1984).
[4] Y. Murakami, Y. Nakajima, K. Otsuka, T. Ohba, R. Matsuo, and K. Ohshima, Mater. Sci. Eng., A **237**, 87 (1997).
[5] Y. Nakajima, S. Aoki, K. Otsuka, and T. Ohba, Mater. Lett. **21**, 271 (1994).
[6] X. Ren and K. Otsuka, Nature (London) **389**, 579 (1997).
[7] X. Ren and K. Otsuka, Mater. Sci. Forum **327-328**, 413 (2000).
[8] J. Janssen, J. Van Humbeeck, M. Chandrasekaran, N. Mwamba, and L. Delaey, J. Phys. Colloq. **43**, Suppl. 12, C4-715 (1982).
[9] J. Deng, X. Ding, T. Lookman, T. Suzuki, K. Otsuka, J. Sun, A. Saxena, and X. Ren, Phys. Rev. B **81**, 220101(R) (2010).
[10] K. Otsuka, X. Ren, Y. Murakami, T. Kawano, T. Ishii, and T. Ohba, Mater. Sci. Eng., A **273-275**, 558 (1999).
[11] M. Parrinello and A. Rahman, Phys. Rev. Lett. **45**, 1196 (1980).
[12] N. Metropolis, A. W. Rosenbluth, M. N. Rosenbluth, A. H. Teller, and E. Teller, J. Chem. Phys. **21**, 1087 (1953).
[13] T. Suzuki and M. Shimono, J. Phys. IV **112**, 129 (2003).

[14] X. Ding, T. Suzuki, J. Sun, X. Ren, and K. Otsuka, Mater. Sci. Eng., A **438-440**, 113 (2006).
[15] X. Ding, T. Suzuki, X. Ren, J. Sun, and K. Otsuka, Phys. Rev. B **74**, 104111 (2006).
[16] M. Shimono, in *Springer Handbook of Materials Measurement Methods*, edited by H. Czichos, T. Saito, and L. Smith (Springer, New York, 2006), pp. 915–952.
[17] Y. Murakami, S. Morito, Y. Nakajima, K. Otsuka, T. Suzuki, and T. Ohba, Mater. Lett. **21**, 275 (1994).
[18] P. A. Flinn and G. M. McManus, Phys. Rev. **124**, 54 (1961).
[19] W. L. Bragg and E. J. Williams, Proc. R. Soc. London, Ser. A **145**, 699 (1934).
[20] J. M. Cowley, Phys. Rev. **77**, 669 (1950).
[21] R. Weinkamer, P. Fratzl, B. Sepiol, and G. Vogl, Phys. Rev. B **58**, 3082 (1998).
[22] L. Zhao, R. Najafabadi, and D. J. Srolovitz, Acta Mater. **44**, 2737 (1996).
[23] H. Mehrer, in *Diffusion in Condensed Matter*, edited by P. Heitjans and J. Karger (Springer, New York, 2005), p. 18.
[24] A. C. Damask and G. J. Dienes, *Point Defects in Metals* (Gordon & Breach, New York, 1963), p. 26.
[25] X. Ren and K. Otsuka, Phys. Rev. Lett. **85**, 1016 (2000).
[26] X. Ding, J. Deng, T. Lookman, T. Suzuki, K. Otsuka, J. Sun, A. Saxena, and X. Ren (unpublished).
[27] L. Zhang and X. Ren, Phys. Rev. B **71**, 174108 (2005).
[28] D. Xue, J. Gao, L. Zhang, H. Bao, W. Liu, C. Zhou, and X. Ren, Appl. Phys. Lett. **94**, 082902 (2009).